Research on Engineering Structures & Materials

journal homepage: http://jresm.org

Research Group

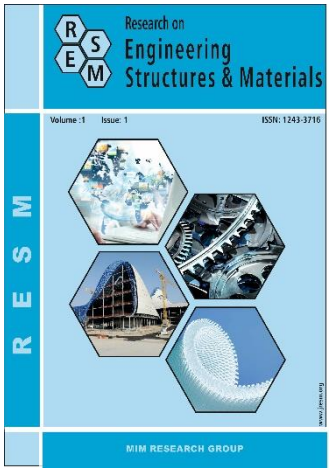

Magnetohydrodynamic squeezing flow of casson nanofluid between two parallel plates in a porous medium using method of matched asymptotic expansion

M. G. Sobamowo

Online Publication Date: 10 Jul 2018
URL: http://dx.doi.org/10.17515/resm2017.46ds0315
DOI: http://dx.doi.org/10.17515/resm2017.46ds0315

Journal Abbreviation: *Res. Eng. Struct. Mat.*

To cite this article

Sobamowo MG. Magnetohydrodynamic squeezing flow of casson nanofluid between two parallel plates in a porous medium using method of matched asymptotic expansion. *Res. Eng. Struct. Mat*., 2018; 4(4-): 257-277.

Research on
Engineering
Structures & Materials
journal homepage: http://jresm.org

RESEARCH GROUP

Research Article

Magnetohydrodynamic squeezing flow of casson nanofluid between two parallel plates in a porous medium using method of matched asymptotic expansion

M. G. Sobamowo

Department of Mechanical Engineering, University of Lagos, Akoka, Lagos, Nigeria

Article Info

Article history:
Received 15 Mar 2018
Revised 11 Apr 2018
Accepted 03 May 2018

Keywords:

Casson fluid, Squeezing flow,
Nanofluid,
Magnetic field, Parallel plates,
Method of Matched Asymptotic Expansion

Abstract

In this paper, unsteady squeezing flow of Casson nanofluid between two parallel plates embedded in a porous medium and subjected to magnetic field is analyzed. The developed systems of partial differential equations for the fluid flow models are converted to ordinary differential equations through suitable similarity variables. The obtained ordinary differential equation is solved using method of matched asymptotic expansion. The accuracies of the approximate analytical method for the small and large values of squeezing numbers are investigated. Good agreements are established between the results of the approximate analytical method and the results numerical method using fourth-fifth order Runge-Kutta-Fehlberg method. Thereafter, the developed approximate analytical solutions are used to investigate the effects of pertinent flow parameters on the squeezing flow phenomena of the nanofluids between the two moving parallel plates. The results established that the as the squeezing number and magnetic field parameters decreases, the flow velocity increases when the plates come together. Also, the velocity of the nanofluids further decreases as the magnetic field parameter increases when the plates move apart. However, the velocity is found to be directly proportional to the nanoparticle concentration during the squeezing flow i.e. when the plates are coming together and an inverse variation between the velocity and nanoparticle concentration is recorded when the plates are moving apart. It is hope that this study will enhance the understanding the phenomena of squeezing flow in various applications.

1. Introduction

The flow characteristics of fluid between two parallel plates have attracted many research interests. This is due to their several applications in engineering such as foodstuff processing, reactor fluidization, moving pistons, chocolate fillers, hydraulic lifts, electric motors, flow inside syringes and nasogastric tubes, compression, and injection, power transmission squeezed film, polymers processing etc. In such fluid flow applications and processes, the analysis of momentum equation is very essential. Following the pioneer work and the basic formulations of squeezing flows under lubrication assumptions by Stefan [1], there have been increasing research interests and many scientific studies on these types of flow. In a past work over some few decades, Reynolds [2] analyzed the squeezing flow between elliptic plates while Archibald [3] investigated the same problem

*Corresponding author: mikegbeminiyi@gmail.com
DOI: http://dx.doi.org/10.17515/resm2017.46ds0315
Res. Eng. Struct. Mat. Vol. 4 Iss. 4 (2018) 257-277

for rectangular plates. The earlier studies on squeezing flows were based on Reynolds equation which its insufficiencies for some cases have been shown by Jackson [4] and Usha and Sridharan [5]. Moreover, the nonlinear behaviours of the flow phenomena have attracted several attempts and renewed research interests aiming at properly analyzing and understanding the squeezing flows [5-14].

Casson fluid is a non-Newtonian fluid first invented by Casson in 1959 [15, 16]. It is a shear thinning liquid which is assumed to have an infinite viscosity at zero rate of shear, a yield stress below which no flow occurs, and a zero viscosity at an infinite rate of shear [17]. It is based on the structure of liquid phase and interactive behaviour of solid of a two-phase suspension. It has ability to capture complex rheological properties of a fluid, unlike other simplified models such as the power law [18] and second, third or fourth-grade models [19]. The non-linear Casson's constitutive equation has been found to describe accurately the flow curves of suspensions of pigments in lithographic varnishes used for preparation of printing inks. In particular, the Casson fluid model describes the flow characteristics of blood more accurately at low shear rates and when it flows through small blood vessels [20]. So, human blood can also be treated as a Casson fluid in the presence of several substances such as fibrinogen, globulin in aqueous base plasma, protein, and human red blood cells. Some famous examples of the Casson fluid include jelly, tomato sauce, honey, soup, concentrated fruit juices etc. Concentrated fluids like sauces, honey, juices, blood, and printing inks can be well described using the Casson model. Many researchers [21-30] studied the Casson fluid under different boundary conditions. Some find the solutions by using either approximate methods or numerical schemes and some find its exact analytical solutions. The solutions when the Casson fluids are in free convection flow with constant wall temperature are also determined. On the other hand, the flow behaviours of the Casson fluid in the presence of magnetic field and heat transfer is also an important research area. Therefore, Khalid et al. [31] focused on the unsteady flow of a Casson fluid past an oscillating vertical plate with constant wall temperature under the non-slip conditions. Application of Casson fluid for flow between two rotating cylinders is performed in [32]. The effect of magnetohydrodynamic (MHD) Casson fluid flow in a lateral direction past linear stretching sheet was explained by Nadeem et al. [33].

In the past and recent studies, different numerical and analytical approximate methods have been adopted to analyze the nonlinearity in the flow process [1-64]. It could be stated that the past efforts in analyzing the squeezing flow problems using approximate analytical methods have been largely based on the applications homotopy analysis method (HAM), Adomain decomposition method (ADM), differential transformation method (DTM), variational iteration method (VIM), variation of parameter method (VPM), optimal homotopy asymptotic method (OHAM) etc. However, the determination of the included unknowns (that will satisfy the second boundary conditions) accompanying the approximate analytical solutions of these methods in analyzing the nonlinear problems increases the computational cost and time. Further, numerical schemes are used for the determination of the unknown included parameters. Practically, this attests that the methods (HAM, ADM, VIM, VPM, DTM, OHAM, DJM, and TAM) can be classified as semi-analytical methods rather than pure approximate analytical methods such as regular, singular and homotopy perturbation methods. Also, these methods (HAM, ADM, VIM, VPM, DTM, OHAM, DJM and TAM) traded off relative simplicity and low computational cost for high accuracy as compared to the perturbation methods. Indisputably, the relatively simple, low cost, highly accurate and total analytic method is still required in analyzing the process and nonlinear equations.

The relative simplicity and low computational cost have made perturbation methods to be widely applied in nonlinear analysis of science, non-science and engineering problems. Although, the validities of the solutions of the traditional perturbation methods are limited to small perturbation parameters and weak nonlinearities, there have been various attempts in recent times to overcome these deficiencies [65-72]. Therefore, over the years, the relative simplicity and high accuracy especially in the limit of small parameter have made perturbation methods interesting tools among the most frequently used approximate analytical methods. Although, perturbation methods provide in general, better results for small perturbation parameters, besides having handy mathematical formulations, they have been shown to have good accuracies, even for relatively large values of the perturbation parameter [65-72]. In the class of the perturbation methods, the method of matched asymptotic expansion (MMAE) is mostly used to determine a uniform and accurate approximation to the solution of singularly perturbed differential equations and to find global properties of differential equations. Moreover, to the best of the author's knowledge, such perturbation method has not been used for the analysis of flow under consideration. Therefore, in this paper, method of matched asymptotic expansion is used to analyze the magnetohydrodynamic squeezing flow of Casson nanofluid between two parallel plates. The developed analytical solutions are used to study the effects of various parameters on the squeezing flow between two parallel plates.

2. Model Development and Analytical Solutions

Consider a Casson nanofluid flowing between two parallel plates placed at time-variant distance and under the influence of magnetic field as shown in the Fig. 1. It is assumed that the flow of the nanofluid is laminar, stable, incompressible, isothermal, non-reacting chemically, the nano-particles and base fluid are in thermal equilibrium and the physical properties are constant. The fluid conducts electrical energy as it flows unsteadily under magnetic force field. The fluid structure is everywhere in thermodynamic equilibrium and the plate is maintained at constant temperature.

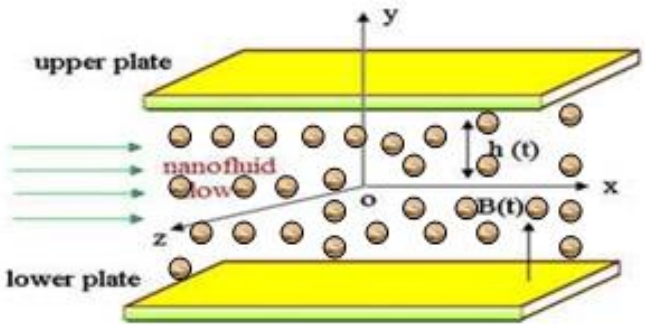

Fig. 1. Model diagram of MHD squeezing flow of nanofluid between two parallel plates embedded in a porous medium

Consider a Casson nanofluid flowing between two parallel plates placed at time-variant distance and under the influence of magnetic field as shown in the Fig. 1. It is assumed that the flow of the nanofluid is laminar, stable, incompressible, isothermal, non-reacting chemically, the nano-particles and base fluid are in thermal equilibrium and the physical properties are constant. The fluid conducts electrical energy as it flows unsteadily under magnetic force field. The fluid structure is everywhere in thermodynamic equilibrium and the plate is maintained at constant temperature.

Using the rheological equation for an isotropic and incompressible Casson fluid, reported by Casson [15,16], is

$$\tau = \tau_0 + \mu\dot{\sigma} \tag{1a}$$

or

$$\tau = \begin{cases} 2\left(\mu_B + \dfrac{p_y}{\sqrt{2\pi}}\right)e_{ij}, & \pi > \pi_c \\ 2\left(\mu_B + \dfrac{p_y}{\sqrt{2\pi_c}}\right)e_{ij}, & \pi_c < \pi \end{cases} \tag{1b}$$

where τ is the shear stress, τ_o is the Casson yield stress, μ is the dynamic viscosity, $\dot{\sigma}$ is the shear rate, $\pi = e_{ij}e_{ij}$ and e_{ij} is the $(i,j)th$ component of the deformation rate, π is the product of the component of deformation rate with itself, π_c is a critical value of this product based on the non-Newtonian model, μ_B the is plastic dynamic viscosity of the non-Newtonian fluid and p_y is the yield stress of the fluid. The velocity as well as the temperature is functions of y, t only. Following the assumptions, the governing equations for the flow are given as

$$\frac{\partial u}{\partial x} + \frac{\partial v}{\partial y} = 0 \tag{2}$$

$$\rho_{nf}\left(\frac{\partial u}{\partial t} + u\frac{\partial u}{\partial x} + v\frac{\partial u}{\partial y}\right) = -\frac{\partial p}{\partial x} + \mu_{nf}\left(1+\frac{1}{\beta}\right)\left(2\frac{\partial^2 u}{\partial x^2} + \frac{\partial^2 u}{\partial x\partial y} + \frac{\partial^2 u}{\partial y^2}\right) - \sigma B_o^2 u - \frac{\mu_{nf} u}{K_p} \tag{3}$$

$$\rho_{nf}\left(\frac{\partial v}{\partial t} + u\frac{\partial v}{\partial x} + v\frac{\partial v}{\partial y}\right) = -\frac{\partial p}{\partial y} + \mu_{nf}\left(1+\frac{1}{\beta}\right)\left(2\frac{\partial v}{\partial x^2} + \frac{\partial^2 v}{\partial x\partial y} + \frac{\partial^2 v}{\partial y^2}\right) - \frac{\mu_{nf} v}{K_p} \tag{4}$$

where

$$\rho_{nf} = \rho_f(1-\phi) + \rho_s\phi \tag{5a}$$

$$\mu_{nf} = \frac{\mu_f}{(1-\phi)^{2.5}} \quad \text{(Brinkman model)} \tag{5b}$$

and the magnetic field parameter is given as

$$B(t) = \frac{B_0}{\sqrt{1-\alpha t}} \tag{6}$$

Under the assumption of no-slip condition, the appropriate boundary conditions are given as

$$y = h(t) = H\sqrt{1-\alpha t}, \quad u = 0, \quad v = -V_w$$
$$y = 0, \quad \frac{\partial u}{\partial y} = 0, \quad v = 0 \tag{7}$$
$$x = 0, \quad u = 0$$

On introducing the following dimensionless and similarity variables

$$u = \frac{\alpha x}{2\sqrt{1-\alpha t}} f'(\eta,t), \quad v = -\frac{\alpha x}{2\sqrt{1-\alpha t}} f(\eta,t), \quad \eta = \frac{y}{H\sqrt{1-\alpha t}}$$
$$Re = -SA(1-\phi)^{2.5} = \frac{\rho_{nf} H V_w}{\mu_{nf}}, \quad S = \frac{\alpha H^2}{2\nu_f}, \quad Da = \frac{K_p}{H^2}, \quad A = (1-\phi) + \phi\frac{\rho_s}{\rho_f} \tag{8}$$

One arrives at

$$\left(1+\frac{1}{\beta}\right) f_{\eta\eta\eta\eta} + Re\left(\eta f_{\eta\eta\eta} + 3 f_{\eta\eta} + f f_{\eta\eta\eta} - f_\eta f_{\eta\eta}\right) - M^2 f_{\eta\eta} - \frac{1}{Da} f_{\eta\eta} = 0 \tag{9a}$$

Alternatively, Eq. (9a) can be written as it can be

$$\left(1+\frac{1}{\beta}\right) f_{\eta\eta\eta\eta} - SA(1-\phi)^{2.5}\left(\eta f_{\eta\eta\eta} + 3 f_{\eta\eta} + f f_{\eta\eta\eta} - f_\eta f_{\eta\eta}\right) - M^2 f_{\eta\eta} - \frac{1}{Da} f_{\eta\eta} = 0 \tag{9b}$$

with the boundary conditions

$$\eta = 0, \quad f = 0, \quad f_{\eta\eta} = 0$$
$$\eta = 1, \quad f = 1, \quad f_\eta = 0 \tag{10}$$

The physical properties of the copper nanoparticles, pure water and kerosene as the base fluids are shown in Table 1.

Table 1: Physical properties of copper nanoparticles, water and kerosene

	Density (kg/m3)	Dynamic viscosity(kg/ms)
Pure water	997.1	0.000891
Kerosene	783.0	0.001640
Copper	8933.0	-

3. Method of Matched Asymptotic Expansion

For small injection and suction at the walls where the permeation Reynolds number is small, the above Eq. (9) can easily be solved using regular perturbation method. It can easily be shown using the regular perturbation method (RPM) that the series solution of Eq. (9), in the absence of magnetic field under a non-porous medium is given as

$$f(\eta)=\frac{\eta}{2}\left(3-\eta^2\right)+\frac{1}{\left(1+\frac{1}{\beta}\right)}Re\left\{\begin{array}{l}\frac{3}{560}\eta^7-\frac{1}{80}\eta^5+\frac{5}{560}\eta^3+\frac{63}{3920}\eta\\+\frac{1}{\left(1+\frac{1}{\beta}\right)}Re\left(\begin{array}{l}\frac{1}{184800}\eta^{11}-\frac{1}{2016}\eta^9+\frac{3}{4900}\eta^7\\+\frac{3}{1400}\eta^5-\frac{3233}{776160}\eta^3+\frac{2459}{1293600}\eta\end{array}\right)\end{array}\right\} \tag{11a}$$

We can also expressed the solution in Eq. (10a) as

$$f(\eta)=\frac{\eta}{2}\left(3-\eta^2\right)-\frac{1}{\left(1+\frac{1}{\beta}\right)}SA(1-\phi)^{2.5}\left\{\begin{array}{l}\frac{3}{560}\eta^7-\frac{1}{80}\eta^5+\frac{5}{560}\eta^3+\frac{63}{3920}\eta\\-\frac{1}{\left(1+\frac{1}{\beta}\right)}SA(1-\phi)^{2.5}\left(\begin{array}{l}\frac{1}{184800}\eta^{11}-\frac{1}{2016}\eta^9+\frac{3}{4900}\eta^7\\+\frac{3}{1400}\eta^5-\frac{3233}{776160}\eta^3+\frac{2459}{1293600}\eta\end{array}\right)\end{array}\right\} \tag{11b}$$

However, for large values of permeation Reynolds number, the solution of the regular perturbation method breaks down. This is because the problem becomes a singular perturbation problem. In order to obtain an analytical solution that is uniformly valid for the whole length of flow, a singular perturbation method, method of matched asymptotic expansion is applied in this work.

Integrating Eq. (9), one arrives at

$$\left(1+\frac{1}{\beta}\right)f_{\eta\eta\eta}+Re\left[\eta f_{\eta\eta}+2f_\eta+ff_{\eta\eta}-\left(f_\eta\right)^2\right]-M^2f_\eta-\frac{1}{Da}f_\eta=\gamma_o \tag{12}$$

where γ_o is space-invariant parameter.

For the purpose of establishing the outer and inner expansions of Eq. (12) subject to the boundary conditions of Eq. (10), Eq. (12) is divided by "*Re*" to have

$$\frac{1}{Re}\left(1+\frac{1}{\beta}\right)f_{\eta\eta\eta}+\eta f_{\eta\eta}+2f_\eta+ff_{\eta\eta}-\left(f_\eta\right)^2-\frac{1}{Re}\left(M^2+\frac{1}{Da}\right)f_\eta=\frac{\gamma_o}{Re} \tag{13}$$

where for large value of $\frac{Re}{\left(1+\frac{1}{\beta}\right)}$, $\frac{1}{Re}\left(1+\frac{1}{\beta}\right)\square\ 1$

Taking $\varepsilon=\frac{1}{Re}\left(1+\frac{1}{\beta}\right)$, Eq. (13) can be written as

$$\varepsilon f_{\eta\eta\eta}+\eta f_{\eta\eta}+2f_\eta+ff_{\eta\eta}-\left(f_\eta\right)^2-\frac{1}{Re}\left(M^2+\frac{1}{Da}\right)f_\eta=\varepsilon\gamma_o \tag{14}$$

For ease of present analysis, Eq. (14) can be re-written as

$$\varepsilon f_{\eta\eta\eta} + \eta f_{\eta\eta} + 2 f_{\eta} + f f_{\eta\eta} - \left(f_{\eta} \right)^2 - \varepsilon^{-\frac{1}{2}} \left[\left(M^2 + \frac{1}{Da} \right) \varepsilon^{\frac{3}{2}} \right] f_{\eta} = -\left[\lambda^2 + \lambda \left[\left(M^2 + \frac{1}{Da} \right) \varepsilon^{\frac{3}{2}} \right] \varepsilon^{-\frac{1}{2}} - 2\lambda \right] \tag{15}$$

Where

$$\varepsilon\gamma_0 = \lambda^2 + \lambda \left[\left(M^2 + \frac{1}{Da} \right) \varepsilon^{\frac{3}{2}} \right] \varepsilon^{-\frac{1}{2}} - 2\lambda$$

Since ε is taken as the small perturbation parameter, it turns out that $\varepsilon^{-\frac{1}{2}} \left[\left(M^2 + \frac{1}{Da} \right) \varepsilon^{\frac{3}{2}} \right] \gg 1$. Therefore, it is established that the term containing a multiple of $\varepsilon^{-\frac{1}{2}} \left[\left(M^2 + \frac{1}{Da} \right) \varepsilon^{\frac{3}{2}} \right]$ will not disappear in the limiting case as $\varepsilon \to 0.$

Since the small perturbation parameter multiplies the highest derivatives as shown in Eq.(15), then the above problem in Eq. (15) is a singular perturbation problem. Method of matched asymptotic expansion is adopted in the present study to provide an approximate analytical solution to the singular perturbation method. The procedures are given as follows.

3.1 The Outer Solution

Assuming that the outer solution takes the form of a series

$$f = f_0 + f_1 \varepsilon^{\frac{1}{2}} + f_2 \varepsilon + f_3 \varepsilon^{\frac{3}{2}} + \ldots \tag{16}$$

and

$$\lambda = \lambda_0 + \lambda_1 \varepsilon^{\frac{1}{2}} + \lambda_2 \varepsilon + \lambda_3 \varepsilon^{\frac{3}{2}} + \ldots \tag{17}$$

where the coefficients λ_i will be determined by matching the outer solutions with the inner solutions.

Substituting Eq. (16) into Eq. (15), after equating the same power of the coefficient ε, one arrives at:

$$\varepsilon^0 : \qquad \left(f_0^{'} \right)^2 - f_0 f_0^{''} = \lambda_0^2 \tag{18a}$$

$$\varepsilon^{\frac{1}{2}} : \qquad 2 f_0^{'} f_1^{'} - f_0 f_1^{''} - f_0 f_1^{''} = 2\lambda_0 \lambda_1 \tag{18b}$$

$$\varepsilon^{1}: \quad 2f_0^{'}f_2^{'}-f_2^{''}f_0-f_2f_0^{''}=-f_0^{'''}-\eta f_{\eta\eta}+2f_{\eta}-\left(f^{'}\right)^2+f_1f_1^{''} +\left(M^2+\frac{1}{Da}\right)f_0^{'}+2\lambda_0\lambda_2+\lambda_1^2+2Re\lambda_1 \tag{18c}$$

$$\varepsilon^{\frac{3}{2}}: \quad 2f_0^{'}f_3^{'}-f_0^{''}f_3-f_0f_3^{''}=-f_1^{'''}-\eta f_{\eta\eta}+2f_{\eta}-Re\left(\eta f_1^{''}+f_1^{'}\right)-f_3^{*}f_0-f_0^{''}f_3-f_1f_2^{*} -f_2f_1^{''}+2f_1f_2^{'}+2f_0^{'}f_3^{'}+\left(M^2+\frac{1}{Da}\right)f_1^{'}+2Re\lambda_1+2\lambda_1\lambda_2 \tag{18d}$$

With the boundary conditions

$$f_0(0)=f_1(0)=f_2(0)=f_3(0)=0$$
$$f_0^{''}(0)=f_1^{''}(0)=f_2^{''}(0)=f_3^{''}(0)=0 \tag{19}$$

It can easily be shown that the solutions of Eqs. (18a-d) using the above boundary conditions in Eq. (18) are

$$f_0(\eta)=\lambda_0\eta, \quad f_1(\eta)=\lambda_1\eta, \quad f_2(\eta)=\lambda_2\eta, \quad f_3(\eta)=\lambda_3\eta \tag{20}$$

Substituting Eq. (19) into Eq. (15) shows that the outer solution of Eq. (15) is given as

$$f=\left(\lambda_0+\lambda_1\varepsilon^{\frac{1}{2}}+\lambda_2\varepsilon+\lambda_3\varepsilon^{\frac{3}{2}}+\ldots\right)\eta \tag{21}$$

The above outer solution given in Eq. (21) is only valid in the region between the edge of the boundary layer and the center distance between the plates

3.2 The Inner Solution

The inner solution can be developed by applying a stretching transformation $\tau=(1-\eta)\varepsilon^{-\frac{1}{2}}$, which implies that

$$\eta=1-\tau\varepsilon^{\frac{1}{2}} \tag{22}$$

Substituting Eq. (22) into Eq. (15), gives

$$\varepsilon^{\frac{3}{2}}Re\left(2\dot{z}+\tau\ddot{z}\right)-\ddot{z}\left(1+\varepsilon Re\right)+\varepsilon^{\frac{1}{2}}\left(\dddot{z}+\left(\dot{z}\right)^2-z\ddot{z}\right)-\sigma\dot{z}=\lambda^2\varepsilon^{\frac{1}{2}}+\lambda\sigma-2Re\lambda\varepsilon^{\frac{3}{2}} \tag{23}$$

Consequently, the inner boundary conditions are given as

$$z(0)=0, \quad \dot{z}(0)=0 \tag{24}$$

where $\sigma=\left(M^2+\frac{1}{Da}\right)\varepsilon^{\frac{3}{2}}$ and the "dot" shows that the derivative is with respect to τ.

One can assume an inner solution of the form that satisfies the boundary conditions,

$$f(\tau)=1+\sum_{n=0}^{\infty}\varepsilon^{\frac{n+1}{2}}z_n(\tau) \tag{25}$$

$$\varepsilon^{\frac{1}{2}}: \qquad \ddot{z}_0+\dot{z}_0=-\frac{\lambda_0}{\sigma} \tag{26a}$$

$$\varepsilon^{1}: \qquad \ddot{z}_1+\dot{z}_1=-\frac{\lambda_1}{\sigma}+\left(\lambda_0-\left(\frac{\lambda_0}{\sigma}\right)^2\right)e^{-\sigma\tau}-\sigma\left(\frac{\lambda_0}{\sigma}\right)^2\tau e^{-\sigma\tau} \tag{26b}$$

$$\varepsilon^{\frac{3}{2}}: \qquad \ddot{z}_2+\dot{z}_2=-\frac{\lambda_2}{\sigma}+\frac{\alpha\lambda_0}{\sigma}e^{-\sigma\tau}+\left(\frac{\lambda_0}{\sigma}\right)^3e^{-2\sigma\tau}+\left[\begin{array}{l}\lambda_1+\lambda_0\sigma(\sigma\tau-2)-\frac{\lambda_0^2}{2\sigma}\left(3\sigma^2\tau^2-2\sigma\tau-2\right)\\ -\frac{2\lambda_0\lambda_1}{\sigma^2}(\sigma\tau+1)+\frac{1}{2}\left(\frac{\lambda_0}{\sigma}\right)^3\left(\sigma^3\tau^3+\sigma^2\tau^2+2\sigma\tau-2\right)\end{array}\right]e^{-\sigma\tau} \tag{26c}$$

The boundary conditions for these inner solutions are given as:

$$z_0(0)=z_1(0)=z_2(0)=\ldots=z_n(0)=0, \qquad \dot{z}_0(0)=\dot{z}_1(0)=\dot{z}_2(0)=\ldots=\dot{z}_n(0)=0 \tag{27}$$

The solutions of Eq. (26a), (26b) and (26c) using the boundary conditions in Eq. (27) are given as

$$z_0=\frac{\lambda_0}{\sigma}\left(1-\sigma\tau-e^{-\sigma\tau}\right) \tag{28a}$$

$$z_1=\frac{\lambda_0}{\sigma}(1-\sigma\tau)+\lambda_0-2\left(\frac{\lambda_0}{\sigma}\right)^2-\left\{\frac{\lambda_1}{\sigma}+\lambda_0(1+\sigma\tau)-\frac{1}{2}\left(\frac{\lambda_0}{\sigma}\right)^2(2+\sigma\tau)^2\right\}e^{-\sigma\tau} \tag{28b}$$

$$\begin{aligned}z_2=&\frac{\lambda_2}{\sigma}(1-\sigma\tau)+\frac{9}{2}\left(\frac{\lambda_0}{\sigma}\right)^3+\lambda_1-\lambda_0\sigma-\frac{\lambda_0^2}{\sigma}-\frac{4\lambda_0\lambda_1}{\sigma^2}+\frac{\lambda_0 Re}{\sigma}-\frac{\lambda_0 Re}{\sigma}(1+\sigma\tau)e^{-\sigma\tau}\\&-\left\{\frac{\lambda_2}{\sigma}+\lambda_1(1+\sigma\tau)+\frac{1}{2}\lambda_0\sigma\left[(\sigma\tau)^2-2\sigma\tau-2\right]\right\}e^{-\sigma\tau}-\frac{\lambda_0^2}{2\sigma}\left[(\sigma\tau)^3+2(\sigma\tau)^2+2\sigma\tau+2\right]\\&-\frac{\lambda_0\lambda_1}{\sigma^2}\left[(\sigma\tau)^2+4\sigma\tau+4\right]+\frac{1}{24}\left(\frac{\lambda_0}{\sigma}\right)^3\left[3(\sigma\tau)^4+16(\sigma\tau)^3+60(\sigma\tau)^2+96\sigma\tau+120\right]e^{-\sigma\tau}\\&+\frac{1}{24}\left(\frac{\lambda_0}{\sigma}\right)^3e^{-2\sigma\tau}\end{aligned} \tag{28c}$$

On substituting Eqs. (28a-28c) into Eq. (25), gives the second-order inner solution which is valid in the boundary layer region as

$$f(\tau)=1+\varepsilon^{\frac{1}{2}}\left\{\begin{array}{l}\left[\frac{\lambda_0}{\sigma}\left(1-\sigma\tau-e^{-\sigma\tau}\right)\right]+\left\{\begin{array}{l}\frac{\lambda_0}{\sigma}(1-\sigma\tau)+\lambda_0-2\left(\frac{\lambda_0}{\sigma}\right)^2\\-\left\{\frac{\lambda_1}{\sigma}+\lambda_0(1+\sigma\tau)-\frac{1}{2}\left(\frac{\lambda_0}{\sigma}\right)^2(2+\sigma\tau)^2\right\}e^{-\sigma\tau}\end{array}\right\}\varepsilon^{\frac{1}{2}}\\+\left\{\begin{array}{l}\frac{\lambda_2}{\sigma}(1-\sigma\tau)+\frac{9}{2}\left(\frac{\lambda_0}{\sigma}\right)^3+\lambda_1-\lambda_0\sigma-\frac{\lambda_0^2}{\sigma}-\frac{4\lambda_0\lambda_1}{\sigma^2}+\frac{\lambda_0 Re}{\sigma}-\frac{\lambda_0 Re}{\sigma}(1+\sigma\tau)e^{-\sigma\tau}\\-\left\{\frac{\lambda_2}{\sigma}+\lambda_1(1+\sigma\tau)+\frac{1}{2}\lambda_0\sigma\left[(\sigma\tau)^2-2\sigma\tau-2\right]\right\}e^{-\sigma\tau}-\frac{\lambda_0^2}{2\sigma}\left[(\sigma\tau)^3+2(\sigma\tau)^2+2\sigma\tau+2\right]\\-\frac{\lambda_0\lambda_1}{\sigma^2}\left[(\sigma\tau)^2+4\sigma\tau+4\right]+\frac{1}{24}\left(\frac{\lambda_0}{\sigma}\right)^3\left[3(\sigma\tau)^4+16(\sigma\tau)^3+60(\sigma\tau)^2+96\sigma\tau+120\right]e^{-\sigma\tau}\\+\frac{1}{24}\left(\frac{\lambda_0}{\sigma}\right)^3e^{-2\sigma\tau}\end{array}\right\}\varepsilon\end{array}\right\} \tag{29}$$

Alternatively, Eq. (29) can be expressed as

$$f(\tau)=1+\varepsilon^{\frac{1}{2}}\left\{\begin{array}{l}\left[\frac{\lambda_0}{\sigma}\left(1-\sigma\tau-e^{-\sigma\tau}\right)\right]+\left\{\begin{array}{l}\frac{\lambda_0}{\sigma}(1-\sigma\tau)+\lambda_0-2\left(\frac{\lambda_0}{\sigma}\right)^2\\-\left\{\frac{\lambda_1}{\sigma}+\lambda_0(1+\sigma\tau)-\frac{1}{2}\left(\frac{\lambda_0}{\sigma}\right)^2(2+\sigma\tau)^2\right\}e^{-\sigma\tau}\end{array}\right\}\varepsilon^{\frac{1}{2}}\\+\left\{\begin{array}{l}\frac{\lambda_2}{\sigma}(1-\sigma\tau)+\frac{9}{2}\left(\frac{\lambda_0}{\sigma}\right)^3+\lambda_1-\lambda_0\sigma-\frac{\lambda_0^2}{\sigma}-\frac{4\lambda_0\lambda_1}{\sigma^2}-\frac{\lambda_0 SA(1-\phi)^{2.5}}{\sigma}+\frac{\lambda_0 SA(1-\phi)^{2.5}}{\sigma}(1+\sigma\tau)e^{-\sigma\tau}\\-\left\{\frac{\lambda_2}{\sigma}+\lambda_1(1+\sigma\tau)+\frac{1}{2}\lambda_0\sigma\left[(\sigma\tau)^2-2\sigma\tau-2\right]\right\}e^{-\sigma\tau}-\frac{\lambda_0^2}{2\sigma}\left[(\sigma\tau)^3+2(\sigma\tau)^2+2\sigma\tau+2\right]\\-\frac{\lambda_0\lambda_1}{\sigma^2}\left[(\sigma\tau)^2+4\sigma\tau+4\right]+\frac{1}{24}\left(\frac{\lambda_0}{\sigma}\right)^3\left[3(\sigma\tau)^4+16(\sigma\tau)^3+60(\sigma\tau)^2+96\sigma\tau+120\right]e^{-\sigma\tau}\\+\frac{1}{24}\left(\frac{\lambda_0}{\sigma}\right)^3e^{-2\sigma\tau}\end{array}\right\}\varepsilon\end{array}\right\} \tag{30}$$

3.2 Matching criteria

The final complete solution can be established by matching the outer solutions with the inner solutions at the edge of the boundary layer i.e. by imposing continuity between the solutions at different scales. This is done to determine the constants or the coefficients λ_i in the outer solution. Expressing the outer solution in terms of the inner variable τ and matching it with the inner solution as $\tau\to\infty$ gives

$$\lambda_0=1,\quad \lambda_1=\frac{1}{\sigma},\quad \lambda_2=1-\frac{1}{\sigma^2} \tag{31}$$

Therefore, the outer solution can be written as

$$f(\eta)=\left\{\lambda_0+\frac{1}{\sigma}\varepsilon^{\frac{1}{2}}+\left(1-\frac{1}{\sigma^2}\right)\varepsilon+\ldots\right\}\eta \tag{32}$$

The complete solution is given by Eqs. (30) and (32). It should be noted the inner solution given by Eq. (30) is valid even outside the boundary layer region i.e. it is uniformly valid throughout the region of $0<\eta<1$.

Another physical quantity of interest in this analysis is the skin friction coefficient, which can be expressed as

$$C_f = \frac{\mu_{nf}\left(1+\frac{1}{\beta}\right)\left(\frac{\partial u}{\partial y}\right)_{y=h(t)}}{\rho_{nf}V_w^2} \tag{33}$$

Using the dimensionless variables in Eq. (8), the dimensionless form of Eq. (33) is given as

$$C_f^* = \frac{H^2}{x^2\left(1-\alpha t\right)Re_x C_f} = \left(1+\frac{1}{\beta}\right)A\left(1-\phi\right)^{2.5}\ f''(1) \tag{34}$$

It should be noted that developed ordinary non-linear differential equation in Eq. (9b) together with the boundary conditions in Eq. (10) was also solved using shooting method coupled with Runge-Kutta-Fehlberg method. The Runge–Kutta–Fehlberg method is an embedded method from the Runge-Kutta family. In the method, the identical function evaluations are used in conjunction with each other to create methods of varying order and similar error constants. By performing one extra calculation, the error in the solution can be estimated and controlled by using the higher-order embedded method that allows for an adaptive step-size to be determined automatically. The Runge-Kutta-Fehlberg is currently the default method in GNU Octave's ode45 solver.

4. Results and Discussion

For the purpose of demonstrating the accuracy of MMAE and RPM, Tables 1-3 show the comparisons of results of the perturbation methods with the results of the numerical methods for different values of permeation Reynolds and Hartmann numbers. In the perturbation methods, it could be established that there is no additional computational cost in the determination of the coefficients or constants of the outer solution. This shows that the cost of computation of approximate analytical solution using the perturbation methods is lower than using the other approximate analytical methods. Although, the solutions of perturbation methods depend on small parameters, its high accuracy within the vicinity of the small perturbation parameters is well established.

Table 2: Comparison of results of flow for large squeezing number in the absence of magnetic field

f	Squeezing	S= 101	M=0, 1/Da=0
η	NM	MMAE	Residue
0.0	0.00000	0.00000	0.00000
0.1	0.16377	0.16414	0.00037
0.2	0.32193	0.32254	0.00061
0.3	0.46995	0.47078	0.00083
0.4	0.60424	0.60523	0.00099
0.5	0.72190	0.72292	0.00102
0.6	0.82063	0.82154	0.00091
0.7	0.89871	0.89938	0.00067
0.8	0.95498	0.95535	0.00037
0.9	0.98878	0.98890	0.00012
1.0	1.00000	1.00000	0.00000

Table 3: Comparison of results for small squeezing number in the absence of magnetic field

f	Squeezing S = 0.5, M=0, 1/Da=0			Squeezing S = 1.5, M=0, 1/Da=0		
η	NM	MMAE	Residue	NM	MMAE	Residue
0.0	0.00000	0.00000	0.00000	0.00000	0.00000	0.00000
0.2	0.31707	0.29170	0.02537	0.31609	0.29880	0.01720
0.4	0.59972	0.57140	0.02832	0.59818	0.57410	0.02408
0.6	0.81886	0.79940	0.01946	0.81747	0.80190	0.01557
0.8	0.95526	0.95690	0.01640	0.95430	0.95800	0.00370
1.0	1.00000	1.00000	0.00000	1.00000	1.00000	0.00000

The results for small and large values of squeezing number are shown in Tables. It could be depicted from the Tables that for small value of squeezing number, the difference between the results of the numerical method (NM) and that of regular perturbation method (RPM) decreases as the squeezing number decreases. Additionally, it is found that the approximate analytical solutions using RPM are practically equivalent to the exact solution for sufficiently small $|S|$. However, regular perturbation solution becomes less reliable and breaks down when the perturbation parameter, S becomes large i.e. the asymptotic error increases as value of the squeezing number increases. This therefore shows that the accuracy of the RPM is commensurate with the smallness of squeezing number. From the analysis, it is established that the solution of the RPM is a fair approximation to the solution of the NM for $-5 \leq S \leq 5$. It should be pointed out that the asymptotic solutions deteriorate when the preceding term is of the same order as proceeding term. i.e. the perturbation solution breaks downs when second term in the asymptotic solution is of the same magnitude with the first term or when the third term in the solution is quantitatively the same as the second term. Although, the method of matched asymptotic expansion gives accurate results for the large values of the permeation squeezing number, it was found that its analytical solution breaks down when

the perturbation parameter, S, is no longer large. Consequently, the error between the NM and MMAE becomes increasing large when S is not large enough for the singular perturbation solutions.

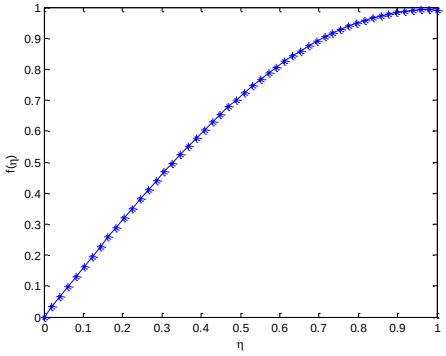

Figure 2a Variation of f(η) with the flow length

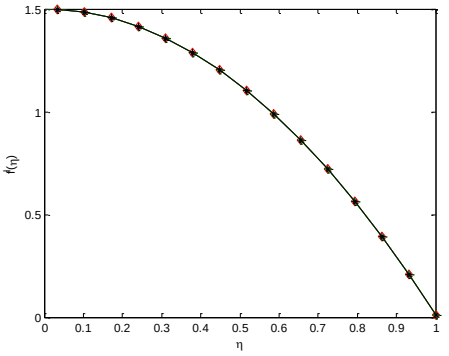

Figure 2b Variation of f'(η) with the flow length

For the value of nanoparticle parameter value, ϕ = 0.15, Figs. 2 and 3 depict the pattern of the flow behavior of the fluid. The figures show that the decrease in the axial velocity of the fluid near the wall region causes an increase in velocity gradient at the wall region. Also, because of the conservativeness of the mass flow rate, the decrease in the fluid velocity near the wall region is compensated by the increasing fluid velocity near the central region.

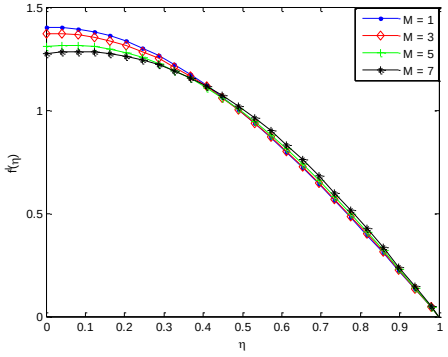

Figure 3 Effects of magnetic number on the velocity of the fluid

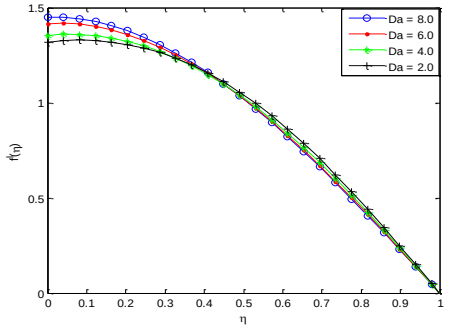

Figure 4 Effects of Darcy number on the velocity

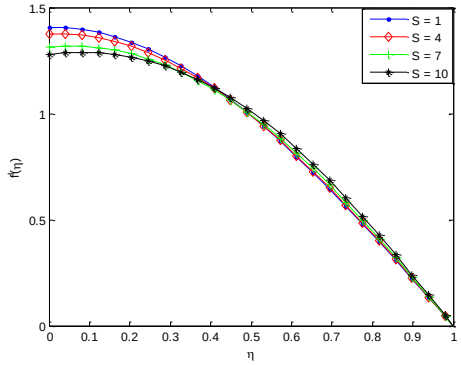

Figure 5 Effects of Squeezing number on the velocity

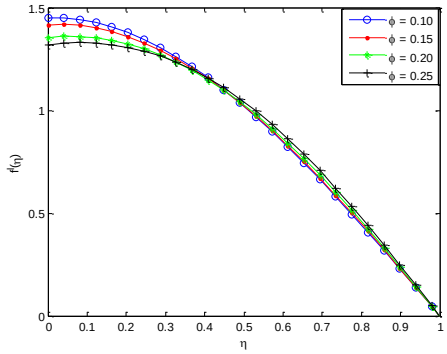

Figure 6 Effects of nanoparticle fraction on the velocity

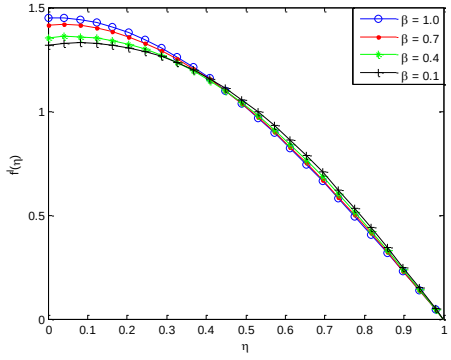

Figure 7 Effects of Casson fluid parameter on the velocity

Fig. 3 which shows the effect of increasing magnetic number or Hartmann parameter (M) on the flow characteristics of the fluid. It is observed that at increasing values of M, the velocity decreases in the range of $0 \leq \eta \leq 0.5$ and then increases in the range $0.5 < \eta \leq 1$. The flow response to the presence of magnetic field is due to the Lorentz force created by the magnetic field which retards the fluid motion at boundary layer during the squeezing flow i.e. when the plates are coming together. It should be noted that during the squeezing flow, especially when the plates are very close to each other, then the flow together with retarding Lorentz force creates adverse pressure gradient. Whenever such forces act over a long time then there might be a point of separation and back flow occurs. The flow velocity of the nanofluids further decreases as the magnetic field parameter increases when the plates move apart. The flow behaviour when the plates move apart are depicted in the figure. This behaviour is as a result of a vacant space occurs and in order not to violate the law of conservation of mass, the fluid in that region moves with high velocity and consequently, an accelerated flow is observed.

Effects of Darcy number on the flow pattern of the Casson nanofluid between the two parallel plates is portrayed in Fig. 4. The figure displays an opposite trend to that of the squeezing number effects on the flow. It could be seen from the figure that as the Darcy number increases, the velocity increases in the range of $0 \leq \eta \leq 0.5$ and then decreases in the range $0.5 < \eta \leq 1$.

Fig. 5 displays the effects of squeezing number on the flow behavior of the fluid. It is clear from the figure that as the squeezing number increases, the velocity decreases in the range of $0 \leq \eta \leq 0.5$ and then increases in the range $0.5 < \eta \leq 1$. Effect of nanoparticle fraction on the fluid velocity is depicted in Fig. 6. The result shows that as the solid volume fraction of the fluid increases the velocity decreases in the range of $0 \leq \eta \leq 0.5$ and then increases in the range $0.5 < \eta \leq 1$. This is because as the nanoparticle volume increases, more collision occurs between nanoparticle and particles with the boundary surface of the plates and consequently the resulting flow retardation which decreases the fluid velocity near the boundary layer. The flow behaviour of the Casson nanofluid to increasing Casson fluid parameter is shown in Fig. 7. The figure depicts the effects of Casson fluid parameter on velocity profile of Casson nanofluid. It is obvious from the figure that Casson the parameter has influence on axial velocity. From the figure, it is clear that the magnitude of velocity of the fluid decreases in the range of $0 \leq \eta \leq 0.5$ and then increases in the range $0.5 < \eta \leq 1$ as the Casson fluid parameter increases.

5. Conclusion

In this work, magnetohydrodynamic squeezing flow of Casson nanofluid between two plates has been analyzed using method of matched asymptotic expansion. The obtained analytical solutions were used to investigate the squeezing phenomena of the nanofluid between the moving plates. Also, the effects of the pertinent flow parameters on the flow process were investigated and discussed. The results of the analytical solutions as developed in this study are good agreement with the results of the numerical method using fourth-fifth order Runge-Kutta-Fehlberg method. The results in this work can be used to further the study of squeezing flow in applications such as power transmission, polymer processing and hydraulic lifts.

Nomenclature

B(t)	Magnetic field strength
Ha	Hartmann parameter
P	Pressure
p_y	Yield stress of the fluid
S	Squeeze Parameter
u	Velocity in x direction
v	Velocity in y Direction
w	Dimensionless velocity in y direction
x	Horizontal axis of flow
y	Perpendicular axis to the flow
k_{nf}	Effective thermal conductivity

Greek Symbol

μ_{nf}	Effective dynamic viscosity
ρ_{nf}	Effective density
η	Dimensionless similarity variable
τ	Hear stress
τ_o	Casson yield stress
μ	Dynamic viscosity
$\dot{\sigma}$	Shear rate
e_{ij}	$(i,j)th$ component of the deformation rate,
π	Product of the component of deformation rate with itself,
π_c	critical value of this product based on the non-Newtonian model,
μ_B	plastic dynamic viscosity of the non-Newtonian fluid

References

[1] M. J. Stefan. Versuch Uber die scheinbare adhesion'', Sitzungsberichte der Akademie der Wissenschaften in Wien. Mathematik-Naturwissen 69, 713–721, 1874.

[2] O. Reynolds. On the theory of lubrication and its application to Mr Beauchamp Tower's experiments, including an experimental determination of the viscosity of olive oil. Philos. Trans. Royal Soc. London 177, 157–234, 1886. https://doi.org/10.1098/rstl.1886.0005

[3] F. R. Archibald, F.R., 1956. Load capacity and time relations for squeeze films. J. Lubr. Technol. 78, A231–A245.

[4] J. D. Jackson. A study of squeezing flow. Appl. Sci. Res. A 11, 148–152, 1962. https://doi.org/10.1007/BF03184719

[5] R. Usha and R. Sridharan, R. Arbitrary squeezing of a viscous fluid between elliptic plates. Fluid Dyn. Res. 18, 35–51, 1996. https://doi.org/10.1016/0169-5983(96)00002-0

[6] Wolfe, W.A., 1965. Squeeze film pressures. Appl. Sci. Res. 14, 77–90. Yang, K.T., 1958. Unsteady laminar boundary layers in an incom- pressible stagnation flow. J. Appl. Math. Trans. ASME 80, 421– 427.

[7] D. C. Kuzma. Fluid inertia effects in squeeze films. Appl. Sci. Res. 18, 15–20, 1968. https://doi.org/10.1007/BF00382330

[8] J. A. Tichy, W. O. Winer. Inertial considerations in parallel circular squeeze film bearings. J. Lubr. Technol. 92, 588–592, 1970. https://doi.org/10.1115/1.3451480

[9] R. J. Grimm. Squeezing flows of Newtonian liquid films: an analysis include the fluid inertia. Appl. Sci. Res. 32 (2), 149–166, 1976. https://doi.org/10.1007/BF00383711

[10] G. Birkhoff. Hydrodynamics, a Study in Logic, Fact and Similitude, Revised ed. Princeton University Press, 137, 1960.

[11] C. Y. Wang. The squeezing of fluid between two plates. J. Appl. Mech. 43 (4), 579–583, 1976. https://doi.org/10.1115/1.3423935

[12] C. Y. Wang, L. T. Watson. Squeezing of a viscous fluid between elliptic plates. Appl. Sci. Res. 35, 195–207, 1979. https://doi.org/10.1007/BF00382705

[13] M. H. Hamdan and R. M. Baron. Analysis of the squeezing flow of dusty fluids. Appl. Sci. Res. 49, 345–354, 1992. https://doi.org/10.1007/BF00419980

[14] P. T. Nhan. Squeeze flow of a viscoelastic solid. J. Non-Newtonian Fluid Mech. 95, 343–362, 2000. https://doi.org/10.1016/S0377-0257(00)00175-0

[15] N. Casson, Rheology of Dispersed System,vol.84,Pergamon Press, Oxford, UK, 1959.

[16]. Casson, N: A flow equation for the pigment oil suspension of the printing ink type. In: Rheology of Disperse Systems, pp. 84-102. Pergamon, New York (1959)

[17] R. K. Dash, K. N. Mehta, and G. Jayaraman, "Casson fluid flow in a pipe filled with a homogeneous porous medium," International Journal of Engineering Science,34(10), 1145–1156, 1996. https://doi.org/10.1016/0020-7225(96)00012-2

[18] H.I.Andersson and B.S.Dandapat,Flow of a power-law fluid over a stretching sheet. Applied Analysis of Continuous Media, 1(339), 1992.

[19] I. M.Sajid, T. A. Hayat and M.Ayub, Unsteadyflow and heat transfer of a second grade fluid over a stretching sheet," Communications in Nonlinear Science and Numerical Simulation,14(1), 96–108, 2009. https://doi.org/10.1016/j.cnsns.2007.07.014

[20] D. A. McDonald. Blood Flows in Arteries, 2nd edn., Chapter 2. Arnold, London (1974)

[21] U. Khan, N. Ahmed, S. I. U. Khan, B. Saima, S. T. Mohyud-din. Unsteady Squeezing flow of Casson fluid between parallel plates. World J. Model. Simul. 10 (4), 308–319, 2014.

[22] M. Mustafa, M, Hayat, T, Pop, I, Aziz, A: Unsteady boundary layer flow of a Casson fluid due to impulsively started moving flat plate. Heat Transf. Asian Res. 40(6), 563-576 (2011) https://doi.org/10.1002/htj.20358

[23]. T. Hayat, S. A. Shehzad, A. Alsaedi, M. S. Alhothuali. Mixed convection stagnation point flow of Casson fluid with convective boundary conditions. Chin. Phys. Lett. 29(11), Article ID 114704 (2012) https://doi.org/10.1088/0256-307X/29/11/114704

[24] S. Mukhopadhyay. Effects of thermal radiation on Casson fluid flow and heat transfer over an unsteady stretching surface subject to suction/blowing. Chin. Phys. B 22(11), Article ID 114702 (2013) https://doi.org/10.1088/1674-1056/22/11/114702

[25] Mukhopadhyay, S, De, PR, Bhattacharyya, K, Layek, GC: Casson fluid flow over an unsteady stretching surface. Ain Shams Eng. J. 4, 933-938 (2013) https://doi.org/10.1016/j.asej.2013.04.004

[26] M. F. Shateyi and W. A. Khanm. Effects of thermal radiation on Casson flow heat and mass transfer around a circular cylinder in porous medium. Eur. Phys. J. Plus 130, 188 (2015) https://doi.org/10.1140/epjp/i2015-15188-y

[27] K. Bhattacharyya. Boundary layer stagnation-point flow of Casson fluid and heat transfer towards a shrinking/stretching sheet. Front. Heat Mass Transf. 4, Article ID 023003 (2013)

[28] S. Pramanik. Casson fluid flow and heat transfer past an exponentially porous stretching surface in presence of thermal radiation. Ain Shams Eng. J. 5, 205-212 (2014) https://doi.org/10.1016/j.asej.2013.05.003

[29] S. Shateyi. A new numerical approach to MHD flow of a Maxwell fluid past a vertical stretching sheet in the presence of thermophoresis and chemical reaction. Bound. Value Probl. 2013, Article ID 196 (2013) https://doi.org/10.1186/1687-2770-2013-196

[30] G. Makanda, S. Shaw, P. Sibanda. Effects of radiation on MHD free convection of a Casson fluid from a horizontal circular cylinder with partial slip in non-Darcy porous medium with viscous dissipation. Bound. Value Probl. 2015, Article ID 75 (2015) https://doi.org/10.1186/s13661-015-0333-5

[31] Khalid, A, Khan, I, Shafie, S: Exact solutions for unsteady free convection flow of Casson fluid over an oscillating vertical plate with constant wall temperature. Abstr. Appl. Anal. 2014, Article ID 946350 (2014)

[32] N. T. M. Eldabe and M. G. E. Salwa, "Heat transfer of mhd non-Newtonian Casson fluid flow between two rotating cylinder," Journal of the Physical Society of Japan,vol.64,p.4164,1995.

[33] S. Nadeem, R. L. Haq, N. S. Akbar, and Z. H. Khan, "MHD three-dimensional Casson fluid flow past a porous linearly stretching sheet", Alexandria. Engineering Journal, Vol. 52, pp. 577582, (2013).

[34] M.M. Rashidi, H. Shahmohamadi and S. Dinarvand, "Analytic approximate solutions for unsteady two dimensional and axisymmetric squeezing flows between parallel plates," Mathematical Problems in Engineering, Vol. (2008), pp. 1-13, 2008.

[35]H.M. Duwairi, B. Tashtoush and R.A. Domesh, "On heat transfer effects of a viscous fluid squeezed and extruded between parallel plates,"Heat Mass Transfer, vol. (14), pp.112-117, 2004.

[36]A. Qayyum, M. Awais, A. Alsaedi and T.Hayat, "Squeezing flow of non-Newtonian second grade fluids and micro polar models, "Chinese Physics Letters, vol. (29), 034701, 2012

[37]M.H Hamdam and R.M. Baron, "Analysis of squeezing flow of dusty fluids," Applied Science Research, 49, 345-354, 1992. https://doi.org/10.1007/BF00419980

[38]M.Mahmood,S.Assghar and M.A. Hossain, "Squeezed flow and heat transfer over a porous surface for viscous fluid," Heat and mass Transfer, 44, 165-173. https://doi.org/10.1007/s00231-006-0218-3

[39]M. Hatami and D.Jing, "Differential Transformation Method for Newtonian and non-Newtonian nanofluids flow analysis: Compared to numerical solution, "Alexandria Engineering Journal, vol. (55), 731-729.

[40] S. T. Mohyud-Din, Z. A. Zaidi, U. Khan, N. Ahmed. On heat and mass transfer analysis for the flow of a nanofluid between rotating parallel plates, Aerospace Science and Technology, 46, 514-522, 2014. https://doi.org/10.1016/j.ast.2015.07.020

[41] S. T. Mohyud-Din, S. I. Khan. Nonlinear radiation effects on squeezing flow of a Casson fluid between parallel disks, Aerospace Science & Technology, Elsevier 48, 186-192, 2016 https://doi.org/10.1016/j.ast.2015.10.019

[42] M. Qayyum, H. Khan, M. T. Rahim, I. Ullah. Modeling and Analysis of Unsteady Axisymmetric Squeezing Fluid Flow through Porous Medium Channel with Slip Boundary. PLoS ONE 10(3), 2015 https://doi.org/10.1371/journal.pone.0117368

[43] M. Qayyum and H. Khan. Behavioral Study of Unsteady Squeezing Flow through Porous Medium, Journal of Porous Media, pp: 83-94, 2016. https://doi.org/10.1615/JPorMedia.v19.i1.60

[44]M. Mustafa, Hayat and S. Obaidat "On heat and mass transfer in the unsteady squeezing flow between parallel plates," Mechanica, vol. (47), pp.1581-1589, 2012.

[45] A.M. Siddiqui, S. Irum, and A.R. Ansari, "Unsteady squeezing flow of viscous MHD fluid between parallel plates," Mathematical Modeling Analysis, vol. (2008), 565-576, 2008.

[46]G. Domairry and A. Aziz, "Approximate analysis of MHD squeeze flow between two parallel disk with suction or injection by homotopy perturbation method," Mathematical Problem in Engineering, 603-616,2009.

[47]N. Acharya, K. Das and P.K. Kundu, "The squeezing flow of Cu-water and Cu-kerosene nanofluid between two parallel plates," Alexandria Engineering Journal, vol. (55), 1177-1186.

[48] N. Ahmed, U. Khan, X. J. Yang, S. I. U. Khan, Z.A. Zaidi, S. T. Mohyud-Din. Magneto hydrodynamic (MHD) squeezing flow of a Casson fluid between parallel disks. Int. J. Phys. Sci. 8 (36), 1788–1799, 2013.

[49] N. Ahmed, U. Khan, Z. A. Zaidi, S. U. Jan, A. Waheed, S. T. Mohyud-Din. MHD Flow of a Dusty Incompressible Fluid between Dilating and Squeezing Porous Walls, Journal of Porous Media, Begal House, 17 (10), 861-867, 2014.

[50] U. Khan, N. Ahmed, S. I. U. Khan, Z. A. Zaidi, X. J. Yang, S. T. Mohyud-Din. On unsteady two-dimensional and axisymmetric squeezing flow between parallel plates. Alexandria Eng. J. 53, 463–468, 2014a. https://doi.org/10.1016/j.aej.2014.02.002

[51] U. Khan, N. Ahmed, Z. A. Zaidi, M. Asadullah, S. T. Mohyud-Din. MHD squeezing flow between two infinite plates. Ain Shams Eng. J. 5, 187–192, 2014b. https://doi.org/10.1016/j.asej.2013.09.007

[52]T. Hayat, A. Yousaf, M. Mustafa and S.Obadiat, "MHD squeezing flow of second grade fluid between parallel disks," International Journal of Numerical Methods, vol. (69), pp.399-410, 2011.

[53] H. Khan, M. Qayyum, O. Khan, and M. Ali. Unsteady Squeezing Flow of Casson Fluid with Magnetohydrodynamic Effect and Passing through Porous Medium," Mathematical Problems in Engineering, vol. 2016, Article ID 4293721, 14 pages, 2016.

[54] I. Ullah, M.T. Rahim, H. Khan, M. Qayyum. Analytical Analysis of Squeezing Flow in Porous Medium with MHD Effect, U.P.B. Sci. Bull., Series A, 78, Iss. 2, 2016.

[55] M. Qayyum, H. Khan, M. T. Rahim, and I. Ullah. Analysis of Unsteady Axisymmetric Squeezing Fluid Flow with Slip and No-Slip Boundaries Using OHAM, Mathematical Problems in Engineering, vol. 2015 (2015). https://doi.org/10.1155/2015/860857

[56] M. Qayyum, H. Khan and O. Khan. Slip Analysis at Fluid-Solid Interface in MHD Squeezing Flow of Casson Fluid through Porous Medium, Results in Physics, 7(2017), 732-750. https://doi.org/10.1016/j.rinp.2017.01.033

[57] O. Khan, M. Qayyum, H. Khan and A. Ali. Improved Analysis for Squeezing of Newtonian Material Between Two Circular Plates, Advances in Materials Science and Engineering, vol. 2017 (2017). https://doi.org/10.1155/2017/5703291

[58] M. Qayyum, H. Khan and M. T. Rahim. A Novel Approach to Approximate Unsteady Squeezing Flow through Porous Medium, Journal of Prime Research in Mathematics, Vol.12 (1) (2016), 91-109.

[59] M.G. Sobamowo and A. T. Akinshilo . On the analysis of squeezing flow of nanofluid between two parallel plates under the influence of magnetic field. Article in Press in Alexandra Engineering Journal. Publication of Elsevier.

[60] M. G. Sobamowo (2017). On the analysis of laminar flow of viscous fluid through a porous channel with suction/injection at slowly expanding or contracting walls. Journal of Computational Applied Mechanics. Vol. 48(2), Article in Press. Journal of Faculty of Engineering, University of Tehran, Iran.

[61] M. G. Sobamowo and L. O. Jayesimi . Squeezing flow analysis of nanofluid under the effects of magnetic field and slip boundary using Chebychev spectral collocation method. Fluid Mechanics, Vol. 3(6)(2017). Article in Press, Science Publishing Group.

[62] M. G. Sobamowo, O. A. Adeleye and J. D. Femi-Oyetoro. Unsteady two-dimensional flow analysis of nanofluid through a porous channel with expanding or contracting walls using Adomian decomposition method. Journal of Engineering Research. Accepted Article. Publication of Faculty of Engineering, University of Lagos, Nigeria, 2017.

[63] A. T. Akinshilo and M. G. Sobamowo. Perturbation Solutions for the Study of MHD Blood as a Third Grade Nanofluid Transporting Gold Nanoparticles through a Porous Channel. Journal of Applied and Computational Mechanics. Vol. 3(2) (2017), 103-113. Publication of Shahid Chamran University of Ahvaz, Iran.

[64] M. G. Sobamowo, L.O. Jayesimi and M. A. Waheed (2017). Magnetohydrodynamic squeezing flow analysis of nanofluid under the effect of slip boundary conditions using variation of parameter. Karbala International Journal of Modern Science. 4(1) (2018), 107-118.

[65] B. Y. Ogunmola, A. T. Akinshilo and M. G. Sobamowo. Perturbation solutions for Hagen-Poiselle flow and Heat transfer of Third-grade fluid with temperature-dependent viscosities and internal heat generation. International Journal of Engineering Mathematics, 2016, Article ID 8915745, 12 pages.

[66] M. G. Sobamowo. Singular perturbation and differential transform methods to two-dimensional flow of nanofluid in a porous channel with expanding/contracting walls subjected to a uniform tranverse magnetic field. Thermal Science and Engineering Progress. 4(2017), 71-84. https://doi.org/10.1016/j.tsep.2017.09.001

[67] U. H. Filobello-Ni-o, Vazquez-Leal, Y. Khan, A. Yildirim, V.M. Jimenez-Fernandez, A. L Herrera May, R. Casta-eda-Sheissa, and J.Cervantes Perez. Perturbation Method and Laplace-Padé

Approximation to solve nonlinear problems. Miskolc Mathematical Notes, 14(1) (2013) 89-101.

[68] U. H. Filobello-Ni-o, Vazquez-Leal, K. Boubaker, Y. Khan, A. Perez-Sesma, A.Sarmiento Reyes, V.M. Jimenez-Fernandez, A Diaz-Sanchez, A. Herrera-May, J. Sanchez-Orea and K. Pereyra-Castro, Perturbation Method as a Powerful Tool to Solve Highly Nonlinear Problems: The Case of Gelfand,s Equation. Asian Journal of Mathematics and Statistics, (2013) 7 pages, DOI: 10.3923 /ajms.2013.

[69] R. Lewandowski. Analysis of strongly non-linear free vibration of beams using perturbation method. Civil and Environmental Reports

[70] Y. K. Cheung, S. H. Chen, S. L. Lau. A modified Lindsteadt-Poincare method for certain strongly non-linear oscillators, International Journal of Non-Linear Mechanics, 26 (1991) 367-378. https://doi.org/10.1016/0020-7462(91)90066-3

[71] C. W. Lim., B. S. Wu. A modified Mickens procedure for certain non-linear oscillators, Journal of Sound and Vibration, 257 (2002) 202-206. https://doi.org/10.1006/jsvi.2001.4233

[72] H. Hu A classical perturbation technique which is valid for large parameters, Journal of Sound and Vibration, 269 (2004) 409-412. https://doi.org/10.1016/S0022-460X(03)00318-3